Dark matter search at colliders and neutrino floor*

Qing-Hong Cao(曹庆宏)[1,2,3;1)] An-Kang Wei(魏安康)[1;2)] Qian-Fei Xiang(向仟飞)[2;3)]

[1]Department of Physics and State Key Laboratory of Nuclear Physics and Technology, Peking University, Beijing 100871, China
[2]Center for High Energy Physics, Peking University, Beijing 100871, China
[3]Collaborative Innovation Center of Quantum Matter, Beijing 100871, China

Abstract: The sensitivity of the direct detection of dark matter (DM) approaches the so-called neutrino floor, below which it is difficult to disentangle the DM candidate from the neutrino background. In this work, we consider the scenario that no DM signals are reported in various DM direct detection experiments and explore whether collider searches could probe DM below the neutrino floor. We adopt several simplified models in which the DM candidate couples to electroweak gauge bosons or leptons in the standard model only through high-dimensional operators. After including the RGE running effect, we investigate the constraints of direct detection, indirect detection, and collider searches. The collider search can probe light DM below the neutrino floor. Particularly, for the effective interaction of $\bar{\chi}\chi B_{\mu\nu}B^{\mu\nu}$, current data from the mono-photon channel at the 13 TeV LHC has already covered the entire parameter space of the neutrino floor.

Keywords: dark matter, collider, direct detection

DOI: 10.1088/1674-1137/abae53

1 Introduction

The existence of dark matter (DM) has been well established by numerous astrophysical and cosmological observations, especially by very precise measurements of the cosmic microwave background (CMB) [1, 2]. The most prevailing and convincing DM candidates are the so-called weakly interacting massive particles (WIMPs). Assuming the standard thermal cosmological history, the WIMPs produced in the early universe through thermal freeze-out naturally afford the observed DM relic density ("WIMP miracle") [3]. Because of their weak interactions with the Standard Model (SM) particles, WIMPs with a mass of approximately 100 GeV would create significant signals in direct and indirect detection experiments, and they could also be produced copiously at high-energy colliders. In the last two decades the precision of DM direct detection experiments has been improved significantly, and it is approaching the "neutrino floor" that is the intrinsic background for DM direct detection [4-8]. However, till now, null results have been reported for every type of dark matter search experiment, and this challenges the WIMP assumptions for DM. As demonstrated in Ref. [9], if the DM candidate couples directly to quarks, the parameter regions to provide the correct relic density are not consistent with the null results of either direct detection, indirect detection, or collider searches. This motivates us to consider the possibility that the DM candidate interacts with electroweak gauge bosons [10-28] or leptons in the SM [29-39].

Rather than focusing on specific DM models, we use an effective-field theory (EFT) approach to parametrize the interactions of the DM candidate and the SM particles at a new physics scale Λ. More specifically, the interactions with gauge bosons are described by dimension-7 operators, while those with leptons are described by dimension-6 operators. The DM candidate is considered to be the only new particle in the energy region relevant for current experiments, and those high-dimensional effective operators are presumably generated by new heavy

Received 30 June 2020, Published online 26 August 2020

* Supported in part by the National Science Foundation of China (11725520, 11675002, 11635001) and in part by the China Postdoctoral Science Foundation (8206300015)

1) E-mail: qinghongcao@pku.edu.cn
2) E-mail: ankangwei@pku.edu.cn
3) E-mail: xiangqf@pku.edu.cn

particles in the dark sector that are substantially heavier than the DM candidate. Even though the DM candidate does not interact directly with quarks in the SM, the quantum effects can induce such interactions and yield a direct detection signal. Hence, an important question in DM direct detection experiments is whether on reaching the neutrino floor one can use other experiments to explore the properties of DM.

An important feature is that energy scales in different experiments vary. For instance, the momentum exchange involved in DM-nucleus recoil is $O(100)$ MeV, while it is $O(100)$ GeV in the LHC searches. Different phenomena are created by operators generated at different energy scales. These operators are related by renormalization group equations (RGE). These loop effects or RGE effects have been widely studied while assuming that DM interacts with gauge bosons [40-43] and leptons [44-47] and that DM interacts with quarks where spin-independent interaction vanishes at tree level [48-51].

In this work, we evolve the RGE from the scale Λ down to the direct detection scale μ_D. Theoretical observations, performed at a corresponding energy scale, are compared with experimental observations. We show that the collider searches can explore some regions under the neutrino floor.

The rest of the paper is organized as follows. In Sec. 2 we give a brief description of DM interactions with electroweak gauge bosons, identify the parameter regions that could overclose the universe, and that could be explored by DM direct detection experiments and LHC searches. In Sec. 3, we repeat the calculations, but for DM interacts with leptons, in that case we also identify parameter regions that could be explored by future electron-positron colliders and DM indirect detection experiments. Finally, we conclude in Sec. 4.

2 Dark matter candidate couples to gauge boson

We start with the case that the DM candidate is a Dirac fermion (χ) and it interacts only with the electroweak gauge bosons in the SM. We first analyze the effective operators that could contribute to the direct detection of DM when gradually evolving from the new physics (NP) scale Λ down to the scale μ_D that is the characteristic energy scale for directly detecting DM.

2.1 Operator analysis

At the level of dimension-5, there are only two operators

$$\bar{\chi}\gamma^{\mu\nu}\chi B_{\mu\nu}, \qquad \bar{\chi}\gamma^{\mu\nu}\chi\tilde{B}_{\mu\nu}, \tag{1}$$

where $\gamma^{\mu\nu}\equiv[\gamma^{\mu},\gamma^{\nu}]/4$ and $B_{\mu\nu}\equiv\partial_{\mu}B_{\nu}-\partial_{\nu}B_{\mu}$ are the field strength tensors of the $U(1)_{\rm Y}$ gauge group. These correspond to the weak magnetic and electric dipoles of DM, respectively, and induce unsuppressed cross sections corrospoding to the annihilation of DM into the $\gamma\gamma$ and γZ modes, yielding a significant line spectrum of cosmic gamma-rays, and thus are tightly constrained by current indirect detection experiments [52]. At the level of dimension-7, there are four scalar-type operators built from $\bar{\chi}\chi$ or $\bar{\chi}\gamma^5\chi$ as follows:

$$\begin{aligned}&\bar{\chi}\chi B_{\mu\nu}B^{\mu\nu}, \qquad \bar{\chi}\chi W^{i}_{\mu\nu}W^{i\mu\nu},\\ &\bar{\chi}\gamma^5\chi B_{\mu\nu}\tilde{B}^{\mu\nu}, \qquad \bar{\chi}\gamma^5\chi W^{i}_{\mu\nu}\tilde{W}^{i\mu\nu},\end{aligned} \tag{2}$$

and six tensor operators constructed from $\bar{\chi}\gamma^{\mu\nu}\chi$, which are

$$\bar{\chi}\gamma^{\mu\nu}\chi B_{\alpha\mu}\tilde{B}^{\alpha\nu}, \quad \bar{\chi}\gamma^{\mu\nu}\chi W^{i}_{\alpha\mu}\tilde{W}^{i\alpha\nu}, \tag{3}$$

and

$$\begin{aligned}&\bar{\chi}\gamma^{\mu\nu}\chi B_{\mu\nu}|\Phi|^2, \qquad \bar{\chi}\gamma^{\mu\nu}\chi\tilde{B}_{\mu\nu}|\Phi|^2,\\ &\bar{\chi}\gamma^{\mu\nu}\chi W_{i\mu\nu}\Phi^{\dagger}\tau^{i}\Phi, \qquad \bar{\chi}\gamma^{\mu\nu}\chi\tilde{W}_{i\mu\nu}\Phi^{\dagger}\tau^{i}\Phi.\end{aligned} \tag{4}$$

Here, $W^{i}_{\mu\nu}\equiv\partial_{\mu}W^{i}_{\nu}-\partial_{\nu}W^{i}_{\mu}+g_2\epsilon^{ijk}W^{j}_{\mu}W^{k}_{\nu}$ is the field-strength tensor of the $SU(2)_{\rm L}$ gauge group and $\tilde{W}^{i\mu\nu}$ is the corresponding dual tensor. The last two operators in Eq. (2) and the two operators in Eq. (3) lead to unsuppressed $\gamma\gamma$ and γZ signals, and the four operators in Eq. (4) induce unsuppressed γh signals, therefore, they are highly constrained and are ignored hereafter. For further discussions and phenomena related to these operators, please refer to Refs. [41, 42, 53]. Finally, we have only the first two operators in Eq. (2), and the Lagrangian can be expressed as

$$\mathcal{L}_{\rm eff}=\frac{C_B}{\Lambda^3}\bar{\chi}\chi B_{\mu\nu}B^{\mu\nu}+\frac{C_W}{\Lambda^3}\bar{\chi}\chi W^{i}_{\mu\nu}W^{i\mu\nu}. \tag{5}$$

They yield velocity-suppressed annihilation cross sections and, therefore, are free from the tight constraint of the gamma ray line spectrum observations [52]. $C_{B,W}$ denotes the Wilson coefficient of the corresponding operator.

We assume that only these two operators are generated at the scale Λ when other new-physics resonances much heavier than Λ are all decoupled. Even though the DM candidate χ and the SM quarks are not directly coupled at the NP scale Λ, they are linked by quantum effects at a lower scale through the RGE running. For example, as shown in Ref. [42], two extra operators that couple the DM candidate to quarks, i.e.

$$O_y=y_q\bar{\chi}\chi\bar{q}\phi q, \qquad O_{\phi}=\bar{\chi}\chi(\phi^{\dagger}\phi)^2, \tag{6}$$

are generated when evolving from Λ down to the weak scale. Here, $y_q=\sqrt{2}m_q/v$ is the Yukawa coupling and v is the vacuum expectation value (VEV) of the SM Higgs doublet ϕ. It is straightforward to show that, to the leading logarithmic (LL) order, the Wilson coefficients of the $O_{y,\phi}$ and $O_{B,W}$ operators are related as follows:

$$C^{q}_{y}(\mu)\simeq\frac{3Y_{qL}Y_{qR}\alpha_1}{\pi}\ln\left(\frac{\mu^2}{\Lambda^2}\right)C_B(\Lambda), \tag{7}$$

$$C_\phi(\mu) \simeq -\frac{9\alpha_1^2}{2}\ln\left(\frac{\mu^2}{\Lambda^2}\right)C_W(\Lambda), \tag{8}$$

where Y_{qL} (Y_{qR}) are the hypercharges of the left-handed (right-handed) quarks assigned as $Y_{uL} = Y_{dL} = 1/6$, $Y_{uR} = 2/3$, and $Y_{dR} = -1/3$. α_1 and α_2 are the gauge coupling constants of the $U(1)_{\rm Y}$ and $SU(2)_{\rm L}$ gauge group, respectively. At the weak scale $\mu_Z(\equiv m_Z)$, $\alpha_1(\mu_Z) \simeq 1/98$, and $\alpha_2(\mu_Z) \simeq 1/29$.

After electroweak symmetry-breaking (EWSB), B_μ and W_μ^3 mix into the photon field A_μ and massive gauge field Z_μ. The effect of Z_μ decouples at the lower scale, below μ_Z, and the relevant operator bases become

$$O_A = \bar{\chi}\chi F_{\mu\nu}F^{\mu\nu},$$

and

$$O_q = m_q\bar{\chi}\chi\bar{q}q. \tag{9}$$

The matching conditions between these two operator bases are

$$\begin{aligned} C_A(\mu_Z) &= c_W^2 C_B(\mu_Z) + s_W^2 C_W(\mu_Z), \\ C_q(\mu_Z) &= C_y^q(\mu_Z) - \frac{v^2}{m_h^2}C_\phi(\mu_Z), \end{aligned} \tag{10}$$

where $c_W \equiv \cos\theta_W$ and $s_W \equiv \sin\theta_W$ are related to the Weinberg angle θ_W.

Next, we further evolve RGEs from μ_Z down to the hadronic scale $\mu_D \sim 1$ GeV at which the DM candidate interacts with the nucleons. O_q will receive contributions from O_A through the exchanging of virtual photons [41]. To LL accuracy,

$$C_q(\mu) \simeq C_q(\mu_Z) + \frac{3Q_q^2\alpha}{\pi}\ln\left(\frac{\mu^2}{\mu_Z^2}\right)C_A(\mu_Z) \tag{11}$$

for $m_q < \mu < \mu_Z$, where Q_q is the electric charge of quarks. During the evolution of RGEs, heavy quarks in the SM are integrated out, yielding an operator

$$O_G = \alpha_s\bar{\chi}\chi G^a_{\mu\nu}G^{a,\mu\nu}, \tag{12}$$

where $G^a_{\mu\nu}$ denotes the field strength of a gluon. The matching condition is given by the simple replacement [54]

$$C_t m_t\bar{\chi}\chi\bar{t}t \to C_G\alpha_s\bar{\chi}\chi G^a_{\mu\nu}G^{a,\mu\nu}, \tag{13}$$

with C_G given at the leading order by

$$C_G(m_t) = -\frac{1}{12\pi}C_t(m_t). \tag{14}$$

Finally, we have the operator basis consisting of O_q, O_A, and O_G. The mixing of O_G with O_q and O_A is subdominant and can be safely ignored. Taking into account the threshold effects at m_b and m_c that contribute to O_G, we obtain the final expressions for the Wilson coefficients as follows:

$$\begin{aligned} C_q(\mu) \simeq& \left(\frac{3Y_{qL}Y_{qR}\alpha_1}{\pi}C_B(\Lambda) + \frac{9\alpha_2^2}{2}\frac{v^2}{m_h^2}C_W(\Lambda)\right)\ln\left(\frac{m_Z^2}{\Lambda^2}\right) \\ &+ \frac{3Q_q^2\alpha}{\pi}C_A(\mu_Z)\ln\left(\frac{\mu_D^2}{m_Z^2}\right), \\ C_G(\mu) \simeq& -\frac{1}{12\pi}\left\{\left(\frac{\alpha_1}{2\pi}C_B(\Lambda) + \frac{27\alpha_2^2}{2}\frac{v^2}{m_h^2}C_W(\Lambda)\right)\ln\left(\frac{m_Z^2}{\Lambda^2}\right)\right. \\ &\left. + \frac{\alpha}{3\pi}C_A(\mu_Z)\left[\ln\left(\frac{m_b^2}{m_Z^2}\right) + 4\ln\left(\frac{m_c^2}{m_Z^2}\right)\right]\right\}. \end{aligned} \tag{15}$$

Figure 1 displays the RGE running of the Wilson coefficients. For simplicity, we consider the operators individually i.e., either $C_W = 0$ (a) or $C_B = 0$ (b) and fix the cut-off scale Λ to be 1000 GeV. In the case of $C_W = 0$, the Wilson coefficients involving the up-type quark (C_y^u) and down-type quark (C_y^d) exhibit opposite signs as the hypercharges of the up-type and down-type quarks are different; see the red and blue curves in the top figure. The sign difference remains unchanged even after the EWSB and matching. However, running from the weak scale μ_Z down to the hadronic scale μ_D, the correction of C_A to C_d is significant and changes the sign of C_d from positive to negative. Conversely, in the case of $C_B = 0$, both the C_u

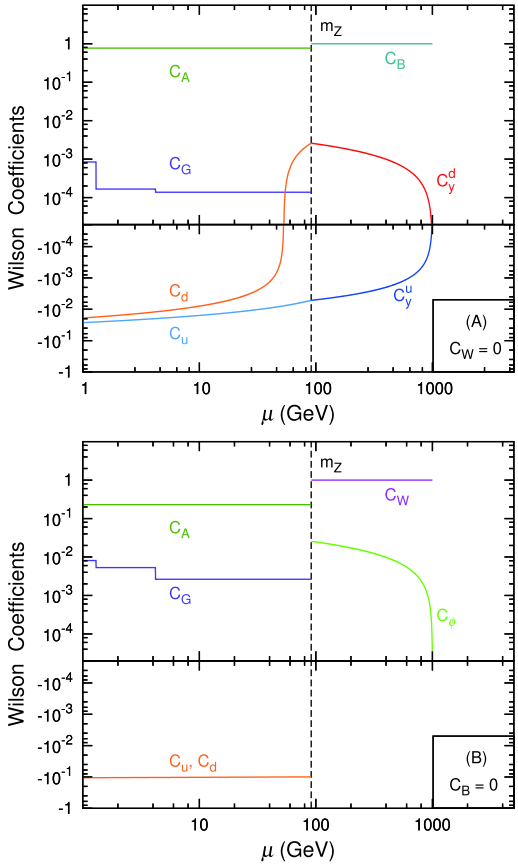

Fig. 1. (color online) Illustrations of running of Wilson coefficients for $C_W = 0$ (a) and $C_B = 0$ (b).

and C_d coefficients receive identical contributions from C_ϕ while the contributions from C_A can be ignored safely; see the bottom figure.

2.2 Experimental searches

As an important approach to probe the DM candidate, the direct detection experiments search for the recoil signals of target nuclei scattered off by incident DM particles. Even though the DM candidate in our model does not interact with quarks directly at the scale Λ, the direct detection signal could be induced at the hadron scale. For example, quantum loop effects induce the interactions of the DM candidate with quarks and gluons, e.g., O_q and O_G in Eqs. (9) and (12) that result in the interaction between the DM candidate and nucleon. In addition, the exchange of two virtual photons will induce an interaction with the entire nucleus, with the interaction strength being proportional to the total electric charge Ze of the nucleus [40].

The contributions of these operators are coherent, leading to the spin-independent (SI) cross section for DM scattering with nuclei [40-42],

$$\sigma_N^{\rm SI} \simeq \frac{m_{\rm red}^2 m_N^2}{\pi\Lambda^6}\left|\frac{\alpha Z^2}{A} f_F^N C_A(\mu_D) + \frac{Z}{A} f_p + \frac{A-Z}{A} f_n\right|^2, \quad (16)$$

where $m_{\rm red}$ is the label of the reduced mass of DM-nuclei system,m_N is the nucleon mass, f_F^N is the form factor for photons, which equals 0.08 (0.12) for the Xenon (Argon) target. The form factor f_N $(N = p,n)$ describes the interactions between the DM candidate and nucleon that are related to the interactions with quarks through

$$f_N = \sum_{q=u,d,s} f_q^N C_q(\mu_D) - \frac{8\pi}{9} f_G^N C_G(\mu_D), \quad (17)$$

where the nucleon form factors f_q^N are given by [55]

$$\begin{aligned} &f_d^p = 0.0191, \quad f_u^p = 0.0153, \quad f_d^n = 0.0273, \\ &f_u^n = 0.0110, \quad f_s^p = f_s^n = 0.0447, \end{aligned} \quad (18)$$

and

$$f_G^N = 1 - \sum_{q=u,d,s} f_q^N. \quad (19)$$

The contributions of the proton and neutron are separated in Eq. (16) as the DM candidate couples differently to them.

Figure 2 displays the constraints on the Wilson coefficients as a function of m_χ at the 90% confidence level (C.L.) using PandaX-II [59], XENON1T [58], and DEAP-3600 [60]. For illustration, we fix the cutoff scale as $\Lambda = 1$ TeV and $C_W = 0$ ($C_B = 0$) in the top (bottom) of Fig. 2, respectively. Both the PandaX-II and XENON1T experiments use the Xenon target; therefore, the contributions of C_A are enhanced by a relatively large Z^2, and

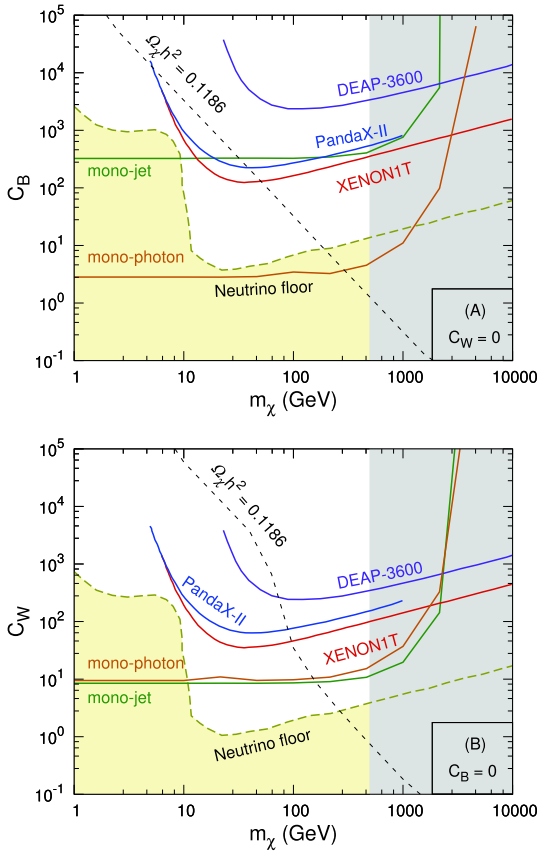

Fig. 2. (color online) Constraints in the m_χ-C_B plane (a) and m_χ-C_W plane (b) with $\Lambda = 1$ TeV. Brown and green solid lines denote the exclusion limits from the mono-photon [56] and mono-jet [57] searches at the 95% confidence level at the 13 TeV LHC. For the SI DM-nucleon scattering, recent bounds from XENON1T [58], PandaX-II [59], and DEAP-3600 [60] are shown. The gray shaded region denotes the parameter space where the EFT is invalid, and it is estimated as $m_\chi > \Lambda/2$. For illustration, the contours of the relic abundance, $\Omega_\chi h^2 = 0.1186$, are also plotted; see the dark dashed curves.

they dominate the contributions of f_p and f_n. Conversely, the contributions of f_p and f_n dominate in the DEAP-3600 experiment that uses an Argon target. For illustration, we plot the contours of the correct relic abundance, $\Omega_\chi h^2 = 0.1186 \pm 0.0020$ [2]; see the Appendix for detailed calculations.

The yellow regions in Fig. 2 denote the so-called neutrino floor that represents the WIMP-discovery limit obtained by assuming an exposure of 1000 ^{8}B neutrinos that are detected on a Xenon target [8]. Recently, a few new methods have been proposed to improve the sensitivity of DM detection beneath the neutrino floor, e.g., using the annual modulation signal [4], directional detection methods [5, 6], or looking for a possible complementarity between different target nuclei [8]. However, the effectiveness of these methods is still limited. It is im-

portant to study whether the collider search can probe the DM candidate below the neutrino floor.

The typical energy of a collider process is $O(100)$ GeV; thus, after EWSB and matching to mass eigenstates, we obtain interactions between quarks and DM that are adopted to calculate the collider observables directly. The processes in the colliders of interest to us are $q\bar{q}\to\chi\bar{\chi}+j$ and $q\bar{q}\to\chi\bar{\chi}+\gamma$, where j denotes a light-flavor jet. The DM candidate often appears as an invisible object in the colliders and yields the signature of missing transverse momentum ($\not{E}_{\rm T}$). The event topology of the two signal processes consists of a large $\not{E}_{\rm T}$ with either a hard jet or a hard photon. The former signature is often termed a "mono-jet" while the latter is termed a "mono-photon." For the model considered in this section, operator O_A will induce a $\rm mono-photon+\not{E}_T$ signal and operator O_q will induce a $\rm mono-jet+\not{E}_T$ signal. To attain the sensitivities of LHC searches, we perform collider simulations of the mono-jet and mono-photon channels. The parton-level events are generated by `MadGraph 5` [61], and `PYTHIA 6` [62] is used to deal with parton showers and hadronization. We adopt `Delphes 3` [63] to carry out a fast detector simulation with a parameter setup for the ATLAS detector.

We follow the procedure of the ATLAS group of the $\rm mono-photon+\not{E}_T$ [56] and $\rm mono-jet+\not{E}_T$ [57] analysis with an integrated luminosity of 36.1 fb^{-1} at the $\sqrt{s}=13$ TeV LHC. Figure 2 presents the exclusion limits derived from the mono-photon search (brown) and the mono-jet search (green) at the LHC. It is difficult to probe directly a DM candidate heavier than about 2 TeV at the LHC as it is limited by the colliding energy. Conversely, when the DM is light, e.g. $m_\chi\lesssim 100$ GeV, the limits are independent of the DM mass as the production cross sections are mainly determined by the effective couplings. Obviously, the collider search has a higher sensitivity than direct detection experiments in regimes where the EFTs are valid, e.g. $m_\chi\lesssim 2$ TeV. We emphasize that the collider searches can probe a light DM ($m_\chi\lesssim 10$ GeV) below the neutrino floor.

In the case of $C_W=0$, the sensitivity of the mono-photon channel is much higher than that of the mono-jet channel, cf. Fig. 2(a). This can be understood as follows. First, the mono-photon signal event can be generated by the O_A and O_q, while the mono-jet signal event can be generated only by the O_q. Note that O_A is directly linked with O_B, while O_q is generated through loop effects and is much smaller than O_A; see Fig. 1(a). Second, the SM background of the mono-photon channel is much cleaner than that of the mono-jet channel, and it yields higher sensitivity to the DM searches at colliders. As a result, the mono-photon channel can cover the entire parameter space of the neutrino floor.

In the case of $C_B=0$, O_A is suppressed by the weak mixing angle after EWSB. Conversely, O_q is slightly enhanced after matching at the weak scale. As a result, the mono-photon and mono-jet channels yield comparable sensitivities to the DM searches; see Fig. 2(b). Even though both channels are better than the DM direct detection experiments, they cannot reach the neutrino floor for $m_\chi\gtrsim 10$ GeV.

3 Dark matter candidate couples to leptons

In this section, we study the scenario of a fermionic DM (χ) interacting only with leptons at the NP scale Λ, termed lepton-philic DM. We assume that the DM candidate χ interacts universally with all the leptons in the SM through

$$\mathcal{L}^l_{\rm eff}=\frac{C_l}{\Lambda^2}\sum_i\bar{\chi}\gamma_\mu\chi\left(\overline{l^i_L}\gamma_\mu l^i_L+\overline{e^i_R}\gamma_\mu e^i_R\right), \tag{20}$$

where the summation over the three generations of leptons in the SM is understood. Again, even though the DM candidate does not directly couple to the SM quarks at scale Λ, the RGE running effects would induce non-zero interactions between the DM candidate and the quarks as follows:

$$\begin{aligned} O^i_q&=\bar{\chi}\gamma^\mu\chi\overline{q^i_L}\gamma_\mu q^i_L,\\ O^i_u&=\bar{\chi}\gamma^\mu\chi\overline{u^i_R}\gamma_\mu u^i_R,\\ O^i_d&=\bar{\chi}\gamma^\mu\chi\overline{d^i_R}\gamma_\mu d^i_R. \end{aligned} \tag{21}$$

Initially, the DM candidate only sees the leptons but is blind to the quarks; however, the connection between the DM candidate and the SM quarks is built through the operator $\bar{\chi}\Gamma^\mu\chi\phi^\dagger i\overleftrightarrow{D}_\mu\phi$ [46, 47].

The strategy of calculating the RGE running effects is similar to that described in the previous section. After matching, the interactions of interest to us are

$$\mathcal{L}\subset\frac{C^V_u}{\Lambda^2}\bar{\chi}\gamma^\mu\chi\bar{u}\gamma_\mu u+\frac{C^V_d}{\Lambda^2}\bar{\chi}\gamma^\mu\chi\bar{d}\gamma_\mu d+\frac{C^V_e}{\Lambda^2}\bar{\chi}\gamma^\mu\chi\bar{e}\gamma_\mu e. \tag{22}$$

In principle, both the Yukawa and gauge interactions would influence the running of RGEs. However, in the case when the DM candidate interacts equally with left-handed and right-handed leptons, the contributions of the Yukawa interactions cancel themselves in each generation [46]. As a result, the induced interactions in Eq. (22) are independent of the quarks' masses and yield identical Wilson coefficients for the three generations. For the sake of simplicity, hereafter, we ignore the index of generation.

We follow Refs. [46, 47] and adopt the package `runDM` [64] to perform a complete RGE running from the NP scale down to the scale of DM direct detection. Figure 3

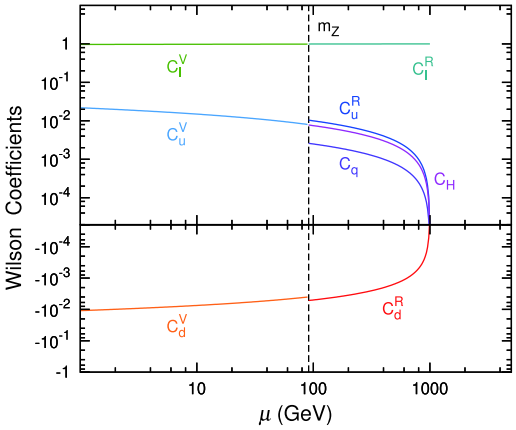

Fig. 3. (color online) RGE running of Wilson coefficients of the effective couplings of χ to the SM fermions.

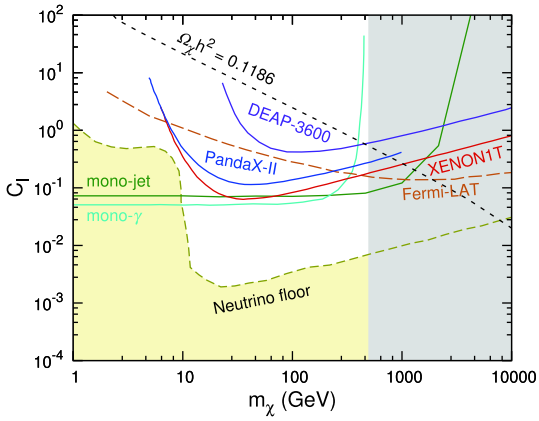

Fig. 4. (color online) The bounds in the m_χ-C_l plane with $\Lambda = 1$ TeV. The brown dashed curve denotes the recent limit from the Fermi-LAT gamma-ray observations of the dwarf galaxies [65], and the cyan solid curve represents the projected sensitivity of the mono-γ channel at the ILC.

displays the Wilson coefficients for different operators. The up-quarks and down-quarks obtain opposite signs with a strength differing by a factor of 2 as the electromagnetic interaction plays the leading role in the RGE running [46].

Equipped with the effective couplings of the DM candidate to the SM quarks, we can discuss the detection of the lepton-philic DM. First, one must consider the direct detection experiment. Owing to the conservation of vector current, the sea quarks and gluons inside nuclei do not contribute. The contributions of all the valence quarks aggregate coherently, leading to the WIMP-nucleus scattering cross sections, as follows:

$$\sigma_N^{\rm SI} = \frac{m_{\rm red}^2}{\pi\Lambda^4}\left|\frac{Z}{A}C_p^V + \frac{A-Z}{A}C_n^V\right|^2. \tag{23}$$

Here, C_p^V and C_n^V denote the interactions of the DM candidate χ with a proton and neutron, respectively. They are related to the effective couplings of χ to the u quark and d quark as follows:

$$C_p^V = 2C_u^V + C_d^V, \qquad C_n^V = C_u^V + 2C_d^V, \tag{24}$$

where C_u^V and C_d^V can be approximated as [46]

$$C_u^V \simeq \frac{4\alpha}{3\pi}C_l, \qquad C_d^V \simeq -\frac{2\alpha}{3\pi}C_l. \tag{25}$$

Therefore, the interaction between $\chi$and the neutron can be safely ignored.

Figure 4 shows the bounds on the Wilson coefficient C_l, at the 90% confidence level, obtained from various direct detection experiments. The yellow shaded region denotes the parameter space below the neutrino floor. Similarly to the case when the DM candidate interacts only with electroweak gauge bosons, the direct detection of the lepton-philic DM cannot touch the neutrino floor. Another method to search for the DM candidate is to examine high-energy cosmic rays, gamma rays, and neutrinos induced by DM decay or annihilation in galactic and extragalactic objects. In the lepton-philic model, the DM candidates predominantly annihilate into a pair of leptons. The constraint on C_l from the indirect search of DM through the cosmic gamma-ray observation by the Fermi-LAT collaboration [65] is plotted in Fig. 4; see the brown dashed curve. Even though the DM will annihilate into all the three-generation leptons, the $\tau^+\tau^-$ channel dominates in the gamma-ray observations as more photons are produced from the τ-lepton decay. Unfortunately, the indirect search experiment also cannot reach the neutrino floor .

The effective couplings of χ to the SM quarks given in Eq. (21) give rise to the mono-jet signal at the LHC; therefore, it yields a strong bound on C_l. See the green curve in Fig. 4. Obviously the LHC will constrain the DM χ with a mass up to about 2 TeV. For $m_\chi \lesssim 10$ GeV, the LHC can probe the parameter space below the neutrino floor.

The lepton-philic DM can be better probed at future electron-positron colliders, e.g. CEPC [66] and ILC [67]. In this work, we explore the potential of the ILC with $\sqrt{s} = 1$ TeV and an integrated luminosity of $1\ {\rm ab}^{-1}$. To identify the mono-γ signal, we require that the signal event contains one energetic photon with energy $E_\gamma > 10$ GeV and $10^\circ < \theta_\gamma < 170^\circ$, where θ_γ is the polar angle between the hard photon and the beam axis. We also require missing mass $m_{\rm miss} > 200$GeV, where the missing mass $m_{\rm miss}$ is defined as $m_{\rm miss} = \sqrt{(p_{e^+} + p_{e^-} - p_\gamma)^2}$ with $p_{e^+}(p_{e^-})$ is the 4-momentum of the initial positron (electron) and p_γ is the 4-momentum of final photon [68]. Note that another searching strategy has been developed recently in Ref. [69] which imposes cuts on $\theta_\gamma - E_\gamma$ plane directly. The cyan solid line in Fig. 4 represents the projected sensitivity of the ILC experiment on C_l. The ILC has a higher sensitivity than the LHC for the DM candidate in the mass re-

gions of interest to us, e.g. $m_\chi \lesssim 200$ GeV; unfortunately, the collider searches cannot reach the neutrino floor for $m_\chi \gtrsim 10$ GeV.

4 Conclusions

With increasing exposures the sensitivity of direct detection of the dark matter (DM) candidate approaches the so-called neutrino floor, below which it is difficult to distinguish the signal induced either by a DM candidate or by a neutrino. In this study, we consider a worst-case scenario that all the direct detection experiments report null results even though the detection sensitivity reaches the neutrino floor. We demonstrate that the collider searches can probe the parameter space under the neutrino floor.

For illustration, we adopt two simplified models in which the DM candidate only couples to electroweak gauge bosons or leptons. Rather than focusing on a specific theoretical model, we use an effective Lagrangian approach to parametrize the interactions of DM with the gauge bosons or the leptons in the SM at a new physics scale $\Lambda$and assume that all other heavy resonances in the UV complete model decouple at the scale Λ. Specifically, we consider two effective Lagrangians as follows:

$$\mathcal{L}^V_{\rm eff} = \frac{C_B}{\Lambda^3}\bar{\chi}\chi B_{\mu\nu}B^{\mu\nu} + \frac{C_W}{\Lambda^3}\bar{\chi}\chi W^i_{\mu\nu}W^{i\mu\nu},$$
$$\mathcal{L}^L_{\rm eff} = \frac{C_l}{\Lambda^2}\sum_i \bar{\chi}\gamma_\mu\chi(\overline{l^i_L}\gamma_\mu l^i_L + \overline{e^i_R}\gamma_\mu e^i_R).$$

Even though the DM candidate does not couple to the SM quarks directly at the scale Λ, it can interact with the quarks and gluons in the SM through the RGE running effects. In this work, we evolve the RGE from high scale Λ to the EWSB scale, match to the basis of mass eigenstates, and then further evolve the RGE down to the direct detection energy scale. For simplicity, we consider the parameters individually and set the other two coefficients to be zero.

We investigate relevant constraints from the direct/indirect detection and collider searches and find that the collider search has higher sensitivity than the direct and indirect detection experiments in the regime where the EFT is valid, e.g. $m_\chi \lesssim 2$ TeV. In all the three simplified models, the collider searches can probe a light DM ($m_\chi \lesssim 10$ GeV) below the neutrino floor. More interestingly, in the case of $C_B \neq 0$ and $C_W = 0$, the current data of the mono-photon channel at the 13 TeV LHC has already covered the entire parameter space of the neutrino floor.

Appendix A: DM annihilation and relic density

The relic abundance predicted by this model should be smaller than the observed quantity reported by the Planck collaboration, $\Omega_\chi h^2 = 0.1186 \pm 0.0020$ [2]. Assuming that DM particles were thermally produced in the early universe, the relic abundance was determined by their thermally averaged annihilation cross sections during the decoupling epoch. If the annihilation cross sections are too small, DM would be overproduced, thereby contradicting the observation.

The evaluation of DM density is performed using the Boltzmann equations. Assuming the standard thermal history of the universe, the DM relic abundance can be parameterized as [3, 70]

$$\Omega_\chi h^2 \simeq \frac{1.04\times10^9\ {\rm GeV}^{-1}(T_0/2.725\ {\rm K})^3 x_f}{M_{\rm pl}\sqrt{g_\star(x_f)}(a+3b/x_f)}, \tag{A1}$$

where $x_f \equiv m_\chi/T_f$; here, T_f denotes the DM freeze-out temperature. $g_\star(x_f)$ represents the effectively relativistic degrees of freedom at the time of the DM freeze-out. $M_{\rm pl}$ is the Planck mass and T_0 is the present CMB temperature. a and b are the coefficients of the velocity expansion of the annihilation cross section $\sigma_{\rm ann}v = a + bv^2 + O(v^4)$. If DM can annihilate into more than one channel, a and b are the total coefficients of all open channels. To calculate the relic density for DM in this work, we should first calculate the a and b coefficients in various annihilation channels.

In this scenario, DM interacts with electroweak gauge bosons and can annihilate to $\gamma\gamma$, ZZ, γZ, and W^+W^-. After EWSB, B_μ , and W^3_μ mix into the photon field A_μ and massive gauge field Z_μ. The effective interactions in terms of physical fields A^μ and Z^μ are

$$\mathcal{L} \supset \frac{C_A}{\Lambda^3}\bar{\chi}\chi F_{\mu\nu}F^{\mu\nu} + \frac{C_{\gamma Z}}{\Lambda^3}\bar{\chi}\chi F_{\mu\nu}Z^{\mu\nu} + \frac{C_{ZZ}}{\Lambda^3}\bar{\chi}\chi Z_{\mu\nu}Z^{\mu\nu} + \frac{C_{W^+W^-}}{\Lambda^3}\bar{\chi}\chi W_{\mu\nu}W^{\mu\nu} \tag{A2}$$

with $F_{\mu\nu} = \partial_\mu A_\nu - \partial_\nu A_\mu$, $Z_{\mu\nu} = \partial_\mu Z_\nu - \partial_\nu Z_\mu$, and $W_{\mu\nu} = \partial_\mu W^+_\nu - \partial_\nu W^-_\mu$. The matching conditions for interactions involving neutral gauge bosons are

$$\begin{aligned} C_A &= C_B c_W^2 + C_W s_W^2, \\ C_{\gamma Z} &= 2 s_W c_W (C_W - C_B), \\ C_{ZZ} &= C_B s_W^2 + C_W c_W^2. \end{aligned} \tag{A3}$$

The interaction with W bosons only originates from $C_W\bar{\chi}\chi W^i_{\mu\nu}W^{i\mu\nu}$, leading to $C_{W^+W^-} = C_W$.

Coefficient a vanishes in each channel and the leading contribution to $\langle\sigma_{\rm ann}v\rangle$ is from the p-wave. The coefficients bs for the annihilation channels of $\chi\chi \to \gamma\gamma$, $\chi\chi \to ZZ$, $\chi\chi \to \gamma Z$, and $\chi\chi \to W^+W^-$ are

$$b_{\chi\chi\to\gamma\gamma} = \frac{C_{\rm A}^2 m_\chi^4}{\pi\Lambda^6},$$
$$b_{\chi\chi\to ZZ} = \frac{C_{ZZ}^2\rho_Z m_\chi^4(8 - 8x_Z + 3x_Z^2)}{8\pi\Lambda^6},$$

$$b_{\chi\chi\to\gamma Z} = \frac{C_{\gamma Z}^2\rho_{\gamma Z}^2(4-x_Z)^2}{32\pi\Lambda^6},$$
$$b_{\chi\chi\to W^+W^-} = \frac{C_{W^+W^-}^2\rho_W m_\chi^4(8-8x_W+3x_W^2)}{4\pi\Lambda^6}, \quad \text{(A4)}$$

where $x_{Z/W}\equiv m_{Z/W}^2/m_\chi^2$, $\rho_{Z/W}\equiv\sqrt{1-m_{Z/W}^2/m_\chi^2}$, and $\rho_{\gamma Z}\equiv\sqrt{1-m_Z^2/4m_\chi^2}$.

Summing over all the annihilation channels and writing the coefficients bs in terms of C_B and C_W, we obtain

$$b_B = \frac{1}{\pi}\frac{m_\chi^4}{\Lambda^6}\left(c_w^4+s_w^4\frac{\rho_Z(8-8x_Z+3x_Z^2)}{8}+\frac{c_w^2s_w^2\beta_{\gamma Z}^2(4-x_Z)^2}{8}\right)C_B^2,$$
$$b_W = \frac{1}{\pi}\frac{m_\chi^4}{\Lambda^6}\left(s_w^4+c_w^4\frac{\rho_Z(8-8x_Z+3x_Z^2)}{8}+\frac{c_w^2s_w^2\beta_{\gamma Z}^2(4-x_Z)^2}{8}+\frac{\rho_W(8-8x_Z+3x_Z^2)}{4}\right)C_W^2,$$
$$b_{BW} = \frac{1}{\pi}\frac{m_\chi^4c_w^2s_w^2}{\Lambda^6}\left(1+\frac{\rho_Z(8-8x_Z+3x_Z^2)}{4}-\frac{\beta_{\gamma Z}^2(4-x_Z)^2}{4}\right)C_BC_W. \quad \text{(A5)}$$

Loop-induced annihilation of quarks and gluons is subdominant and can be safely ignored. It is known that when $C_W=0$, the annihilation channel of $\gamma\gamma$ always dominates and the constraint on C_B is roughly proportional to the inverse of m_χ^2. In contrast, in the case $C_B=0$, the annihilation channel of γZ or W^+W^- will dominate once the channel opens, explaining the behavior of the relic density curve with m_χ around 80 GeV in Fig. 2(b).

In the case when the DM candidate interacts with leptons, DM decays to leptons directly with a and b coefficients given by

$$a = \frac{1}{2\pi\Lambda^4}\sum_l C_l^2\rho_l(2m_\chi^2+m_l^2), \quad \text{(A6)}$$

$$b = \frac{1}{2\pi\Lambda^4}\sum_l C_l^2\rho_l(2m_\chi^2+m_l^2)\frac{-4+2m_f^2/m_\chi^2+11m_f^4/m_\chi^4}{24(1-m_f^2/m_\chi^2)(2+m_f^2/m_\chi^2)}. \quad \text{(A7)}$$

Here, the summing is performed for all lepton flavors.

References

1 **WMAP** Collaboration, G. Hinshaw *et al.*, Astrophys. J. Suppl., **208**: 19 (2013), arXiv:1212.5226
2 **Planck** Collaboration, N. Aghanim *et al.*, *Planck 2018 results. VI. Cosmological parameters*, arXiv: 1807.06209.
3 G. Jungman, M. Kamionkowski, and K. Griest, Phys. Rept., **267**: 195-373 (1996), arXiv:hep-ph/9506380
4 K. Freese, M. Lisanti, and C. Savage, Rev. Mod. Phys., **85**: 1561-1581 (2013), arXiv:1209.3339
5 S. Ahlen *et al.*, Int. J. Mod. Phys. A, **25**: 1-51 (2010), arXiv:0911.0323
6 P. Grothaus, M. Fairbairn, and J. Monroe, Phys. Rev. D, **90**(5): 055018 (2014), arXiv:1406.5047
7 J. Billard, L. Strigari, and E. Figueroa-Feliciano, Phys. Rev. D, **89**(2): 023524 (2014), arXiv:1307.5458
8 F. Ruppin, J. Billard, E. Figueroa-Feliciano *et al.*, Phys. Rev. D, **90**(8): 083510 (2014), arXiv:1408.3581
9 K. Cheung, P.-Y. Tseng, Y.-L. S. Tsai *et al.*, JCAP, **1205**: 001 (2012), arXiv:1201.3402
10 M. Cirelli, N. Fornengo, and A. Strumia, Nucl. Phys. B, **753**: 178-194 (2006), arXiv:hep-ph/0512090
11 M. Cirelli and A. Strumia, New J. Phys., **11**: 105005 (2009), arXiv:0903.3381
12 Y. Cai, W. Chao, and S. Yang, JHEP, **12**: 043 (2012), arXiv:1208.3949
13 C. Cai, Z.-M. Huang, Z. Kang *et al.*, Phys. Rev. D, **92**(11): 115004 (2015), arXiv:1510.01559
14 T. Cohen, J. Kearney, A. Pierce *et al.*, Phys. Rev. D, **85**: 075003 (2012), arXiv:1109.2604
15 O. Fischer and J. J. van der Bij, JCAP, **1401**: 032 (2014), arXiv:1311.1077
16 A. Dedes and D. Karamitros, Phys. Rev. D, **89**(11): 115002 (2014), arXiv:1403.7744
17 M. A. Fedderke, T. Lin, and L.-T. Wang, *Probing the fermionic Higgs portal at lepton colliders*, arXiv: 1506.05465
18 L. Calibbi, A. Mariotti, and P. Tziveloglou, JHEP, **10**: 116 (2015), arXiv:1505.03867
19 C. E. Yaguna, Phys. Rev. D, **92**(11): 115002 (2015), arXiv:1510.06151
20 T. M. P. Tait and Z.-H. Yu, JHEP, **03**: 204 (2016), arXiv:1601.01354
21 S. Horiuchi, O. Macias, D. Restrepo *et al.*, JCAP, **1603**(03): 048 (2016), arXiv:1602.04788
22 C. Cai, Z.-H. Yu, and H.-H. Zhang, CEPC *Precision of Electroweak Oblique Parameters and Weakly Interacting Dark Matter: the Fermionic Case*, arXiv: 1611.02186
23 T. Abe, *Effect of CP violation in the singlet-doublet dark matter model*, arXiv: 1702.07236
24 C. Cai, Z.-H. Yu, and H.-H. Zhang, *CEPC Precision of Electroweak Oblique Parameters and Weakly Interacting Dark Matter: the Scalar Case*, arXiv: 1705.07921
25 Q.-F. Xiang, X.-J. Bi, P.-F. Yin *et al.*, Phys. Rev. D, **97**(5): 055004 (2018), arXiv:1707.03094
26 J.-W. Wang, X.-J. Bi, Q.-F. Xiang *et al.*, Phys. Rev. D, **97**(3): 035021 (2018), arXiv:1711.05622
27 Q.-H. Cao, T. Gong, K.-P. Xie *et al.*, Sci. China Phys. Mech. Astron., **62**(8): 981011 (2019), arXiv:1810.07658
28 C. Arina, A. Cheek, K. Mimasu *et al.*, *Light and Darkness: consistently coupling dark matter to photons via effective operators*, arXiv: 2005.12789
29 L. Bergstrom, T. Bringmann, and J. Edsjo, Phys.Rev. D, **78**: 103520 (2008), arXiv:0808.3725
30 V. Barger, W. Y. Keung, D. Marfatia *et al.*, Phys.Lett. B, **672**: 141-146 (2009), arXiv:0809.0162
31 M. Cirelli, M. Kadastik, M. Raidal *et al.*, Nucl.Phys. B, **813**: 1-21 (2009), arXiv:0809.2409
32 P.-f. Yin, Q. Yuan, J. Liu *et al.*, Phys.Rev. D, **79**: 023512 (2009), arXiv:0811.0176
33 J. Zhang, X.-J. Bi, J. Liu *et al.*, Phys.Rev. D, **80**: 023007 (2009), arXiv:0812.0522
34 P. J. Fox and E. Poppitz, Phys. Rev. D, **79**: 083528 (2009),

arXiv:0811.0399
35 L. Bergstrom, J. Edsjo, and G. Zaharijas, Phys.Rev.Lett., **103**: 031103 (2009), arXiv:0905.0333
36 Q.-H. Cao, E. Ma, and G. Shaughnessy, Phys. Lett. B, **673**: 152-155 (2009), arXiv:0901.1334
37 A. Ibarra, A. Ringwald, D. Tran *et al*., JCAP, **0908**: 017 (2009), arXiv:0903.3625
38 S.-J. Lin, Q. Yuan, and X.-J. Bi, Phys. Rev. D, **91**(6): 063508 (2015), arXiv:1409.6248
39 Q.-F. Xiang, X.-J. Bi, S.-J. Lin *et al*., Phys. Lett. B, **773**: 448-454 (2017), arXiv:1707.09313
40 N. Weiner and I. Yavin, Phys. Rev. D, **86**: 075021 (2012), arXiv:1206.2910
41 M. T. Frandsen, U. Haisch, F. Kahlhoefer *et al*., JCAP, **1210**: 033 (2012), arXiv:1207.3971
42 A. Crivellin and U. Haisch, Phys. Rev. D, **90**: 115011 (2014), arXiv:1408.5046
43 B. J. Kavanagh, P. Panci, and R. Ziegler, JHEP, **04**: 089 (2019), arXiv:1810.00033
44 J. Kopp, V. Niro, T. Schwetz *et al*., Phys. Rev. D, **80**: 083502 (2009), arXiv:0907.3159
45 P. J. Fox, R. Harnik, J. Kopp *et al*., Phys. Rev. D, **84**: 014028 (2011), arXiv:1103.0240
46 F. D'Eramo, B. J. Kavanagh, and P. Panci, JHEP, **08**: 111 (2016), arXiv:1605.04917
47 F. D 'Eramo and M. Procura, JHEP, **04**: 054 (2015), arXiv:1411.3342
48 T. Han, H. Liu, S. Mukhopadhyay *et al*., JHEP, **03**: 080 (2019), arXiv:1810.04679
49 D. Azevedo, M. Duch, B. Grzadkowski *et al*., JHEP, **01**: 138 (2019), arXiv:1810.06105
50 K. Ghorbani and P. H. Ghorbani, JHEP, **05**: 096 (2019), arXiv:1812.04092
51 K. A. Mohan, D. Sengupta, T. M. Tait *et al*., JHEP, **05**: 115 (2019), arXiv:1903.05650
52 **Fermi-LAT** Collaboration, M. Ackermann *et al*., Phys. Rev. D, **91**(12): 122002 (2015), arXiv:1506.00013
53 A. Rajaraman, T. M. P. Tait, and D. Whiteson, JCAP, **1209**: 003 (2012), arXiv:1205.4723
54 M. A. Shifman, A. I. Vainshtein, and V. I. Zakharov, Phys. Lett. B, **78**: 443-446 (1978)
55 G. Belanger, F. Boudjema, A. Pukhov *et al*., Comput. Phys. Commun., **185**: 960-985 (2014), arXiv:1305.0237
56 **ATLAS** Collaboration, M. Aaboud *et al*., Eur. Phys. J. C, **77**(6): 393 (2017), arXiv:1704.03848
57 **ATLAS** Collaboration, M. Aaboud *et al*., JHEP, **01**: 126 (2018), arXiv:1711.03301
58 **XENON** Collaboration, E. Aprile *et al*., Phys. Rev. Lett., **119**(18): 181301 (2017), arXiv:1705.06655
59 **PandaX-Ⅱ** Collaboration, A. Tan *et al*., Phys. Rev. Lett., **117**(12): 121303 (2016), arXiv:1607.07400
60 **DEAP** Collaboration, R. Ajaj *et al*., Phys. Rev. D, **100**(2): 022004 (2019), arXiv:1902.04048
61 J. Alwall, R. Frederix, S. Frixione *et al*., JHEP, **07**: 079 (2014), arXiv:1405.0301
62 T. Sjostrand, S. Mrenna, and P. Z. Skands, JHEP, **0605**: 026 (2006), arXiv:hep-ph/0603175
63 **DELPHES 3** Collaboration, J. de Favereau, C. Delaere, P. Demin *et al*., JHEP, **02**: 057 (2014), arXiv:1307.6346
64 P. P. F. D 'Eramo, B. J. Kavanagh, *runDM* (*Version 1.0*)[*Computer software*], doi: *10.5281/zenodo.823249*. Available at *https://github.com/bradkav/runDM/*
65 **Fermi-LAT** Collaboration, M. Ackermann *et al*., Phys. Rev. Lett., **115**(23): 231301 (2015), arXiv:1503.02641
66 **CEPC Study Group** Collaboration, M. Dong *et al*., *CEPC Conceptual Design Report: Volume 2 - Physics & Detector*, arXiv: 1811.10545
67 H. Baer, T. Barklow, K. Fujii *et al*., *The International Linear Collider Technical Design Report - Volume 2: Physics*, arXiv: 1306.6352
68 Z.-H. Yu, Q.-S. Yan, and P.-F. Yin, Phys. Rev. D, **88**(7): 075015 (2013), arXiv:1307.5740
69 Z. Liu, Y.-H. Xu, and Y. Zhang, JHEP, **06**: 009 (2019), arXiv:1903.12114
70 E. W. Kolb and M. S. Turner, Front. Phys., **69**: 1-547 (1990)